IAEA
INTERNATIONAL ATOMIC ENERGY AGENCY

20th IAEA Fusion Energy Conference

Vilamoura, Portugal, 1-6 November 2004

IAEA-CN-116 / EX / 7-2

Active Control of MHD Instabilities by ECCD in ASDEX Upgrade

M.Maraschek[1], G.Gantenbein[2], T.P.Goodman[3], S.Günter[1], D.F. Howell[4], F.Leuterer[1], A.Mück[1], O.Sauter[3], H.Zohm[1], contributors to the EFDA-JET workprogramme[5] and the ASDEX Upgrade Team

[1]Max-Planck-Institut für Plasmaphysik, EURATOM Association, D-85748 Garching
[2]Institut für Plasmaforschung, Pfaffenwaldring 31, D-70569 Stuttgart
[3]CRPP - EPFL, EURATOM Association, CH-1015 Lausanne, Switzerland
[4]Euratom Association/UKAEA, Culham Science Centre, Abingdon, United Kingdom
[5]see annex 1 of J.Pamela et al., Nucl. Fusion **43** (2003) 1540

Active Control of MHD Instabilities by ECCD in ASDEX Upgrade

M.Maraschek[1], G.Gantenbein[2], T.P.Goodman[3], S.Günter[1], D.F. Howell[4], F.Leuterer[1], A.Mück[1], O.Sauter[3], H.Zohm[1], contributors to the EFDA-JET workprogramme[5] and the ASDEX Upgrade Team

[1]Max-Planck-Institut für Plasmaphysik, EURATOM Association, D-85748 Garching
[2]Institut für Plasmaforschung, Pfaffenwaldring 31, D-70569 Stuttgart
[3]CRPP - EPFL, EURATOM Association, CH-1015 Lausanne, Switzerland
[4]Euratom Association/UKAEA, Culham Science Centre, Abingdon, United Kingdom
[5]see annex 1 of J.Pamela et al., Nucl. Fusion **43** (2003) 1540
e-mail: Maraschek@ipp.mpg.de

Abstract The modification of the stability and the behaviour of core MHD with local electron cyclotron current drive (ECCD) is presented. Starting from the inner most resonant surface, the $q = 1$ surface, the stability and hence the repetition rate and size of sawteeth is controlled with local on/off-axis co/counter-ECCD. The sawteeth themself can serve as a trigger for neoclassical tearing modes (NTM) and therefore the excitation of NTMs can be influenced. Once these NTMs get excited they can be fully stabilised at high β_N with co-ECCD at the resonant surface. Detailed experiments on the dependence of the stabilisation on the ECCD deposition width and the total driven current have been shown to improve the stabilisation efficiency both for the (3/2) and the (2/1)-NTM significantly. In the presence of (3/2)-NTMs the impact on the confinement can be reduced by triggering the so-called frequently interrupted regime (FIR-NTM) with current drive in the vicinity of the (4/3) surface leading also to clearer understanding of the FIR-NTM.

1. Introduction

Core MHD activity is of general interest for the overall performance of fusion experiments and in particular for ITER or a later fusion reactor. On the one hand sawteeth with a moderate size are beneficial to control the helium ash removal from the plasma and to avoid central impurity accumulation. On the other hand large sawteeth with a low repetition frequency can trigger so-called neoclassical tearing modes (NTMs). An external control of the sawtooth size and repetition rate (τ_{st} = time between two subsequent sawteeth) is therefore highly desired.

NTMs appear only in discharges with high normalised pressure $\beta_N = \beta_t/(I_p/aB_t)$. The flattening of the pressure profile over the island (due to high parallel heat transport, $\chi_{||} >> \chi_{\perp}$) leads to a hole in the bootstrap current profile, which is the main drive for an NTM. The (3/2)-NTM reduces the achievable β at least in the order of 10%-20%. Since for the fusion power $P_{fus} \propto \beta^2$ holds, this loss is significant for a fusion reactor. A (2/1)-NTM leads to an even larger loss in confinement and the possible mode locking may even cause disruptions for low q_{95} values. Therefore the control of core MHD with the ability to trigger or suppress NTMs and the removal or, if this is not possible, mitigation of the confinement reduction is very important. Ideally this should all be done automatically by the tokamak control system. The ECCD is well suited for this purpose due to its narrow deposition and the possibility to exactly control of the deposition radius.

2. Sawtooth tailoring

2.1. Sawtooth de / stabilisation with ECCD Sawteeth play a significant role for the central particle and energy confinement in two different aspects. The presence, size, repetition rate or absence of sawteeth modify the central confinement and play a crucial role for the core helium ash removal. On the other hand sawteeth can create a seed-island for the excitation of NTMs. By reducing the size of the sawteeth (destabilisation of sawteeth, reduction of τ_{st}) or suppressing them totally (stabilisation of sawteeth, increase of $\tau_{st} \to \infty$) the excitation of an NTM can be avoided on ASDEX Upgrade. One way to modify τ_{st} is the use of different NBI sources with different tangency radius and hence deposition profile leading also to a flattening of the q-profile [1,2]. A variation in the distribution of fast particles should also play a role here.

The influence of co-current drive (co-ECCD), counter-current drive (counter-ECCD) and pure ECRH heating on the sawtooth repetition rate τ_{st} has been investigated in detail. By a variation of the toroidal launching angle of the ECCD antennas pure heating, counter- and co-ECCD can be achieved. Conventional H-mode discharges in deuterium with low triangularity δ, monotonic q-profiles with $I_p = 0.8MA$ and densities in the order of $\bar{n}_e \approx 6 \cdot 10^{19} m^{-3}$ have been used. Only 5 MW of NBI heating power have been applied, in order to keep β_N low and to avoid triggering NTMs by sawteeth. In these discharges the magnetic field has been ramped within individual shots and on a shot to shot base in a range from $B_t \approx -2.65T$ up to $B_t \approx -2.05T$. This results in a variation of the ECRH deposition from $\rho_{pol} \approx -0.6$ ($\rho_{pol} < 0$ for the high field side (HFS) of the plasma) up to $\rho_{pol} \approx 0.3$ ($\rho_{pol} > 0$ for the low field side (LFS)). The second harmonic X-mode resonance is located in the plasma centre for $-2.5T$. The ECRH and ECCD power of $P_{ECH} \approx 0.8MW$ is typically 15% of the NBI power. The deposition radius of the ECRH and ECCD is calculated with the TORBEAM beam tracing code [3].

For co-ECCD at $\rho_{pol} = -0.42$ (HFS) the longest sawtooth repetition rate $\tau_{st} \approx 320ms$ can be observed, whereas for depositions inside the sawtooth inversion radius a reduction to $\tau_{st} \approx 50ms$ can be measured. During power scans from 0MW to 0.8MW of co-ECCD inside the inversion radius a clear decrease of τ_{st} with the power could be observed. With the B_t field corresponding to a deposition at $\rho_{pol} = -0.42$ a complete sawtooth stabilisation for the maximal ECRH pulse of 2s could be achieved. During this phase fishbone activity appears. The driven co-current inside / outside the inversion radius typically steepens / flattens the q-profile in the vicinity of $q = 1$ and hence increases / decreases $q\prime$ [4]. The increase / decrease of $q\prime$ is expected to destabilise / stabilise sawteeth, leading to a decrease / increase of τ_{st} and decrease / increase of the sawtooth size, estimated by the variation of T_e, consistently with the observations.

For counter-ECCD the magnetic field scan shows a different picture. Inside the inversion radius and in the centre a broad range with stabilisation is observed, reaching $\tau_{st} \approx 800ms$. For central deposition with fixed field a complete stabilisation is observed. With central counter-ECCD a power threshold for complete sawtooth suppression is observed below which τ_{st} remains nearly constant ($\tau_{st} \approx 60ms...90ms$). Above this threshold a clear continuous (1/1) mode without fishbones is present, while the sawteeth are fully suppressed. In the phase before the suppression of the sawteeth, the size of the (1/1) activity increases continuously with power. This (1/1) mode causes an increased continuous transport, so that no impurity accumulation in this phase is observed (constant level of soft X-ray radiation from the centre). This (1/1) activity is a clear difference between off-axis co-ECCD and on-axis counter-ECCD for the sawtooth suppression. For further off-axis counter-ECCD power, $P_{ECCD} \approx 1.7MW$, τ_{st} could be reduced to values from $110ms$ to $70ms$. It can be concluded, that the combination of the destabilisation of the (1/1) mode together with a minimum q of unity with reversed shear and q-profile can lead to the observed sawtooth suppression here.

In order to achieve identical deposition profiles for the pure heating case we did not use $0°$ launching angle for the ECRH, but 50% co-ECCD and 50% counter-ECCD at $\pm 15°$ has been used at the same time. The heating itself leads to an additional small co-current due to the increased conductivity of the heating. The behaviour of τ_{st} as a function of the resulting deposition radius is very similar, but less pronounced as for the co-ECCD case. For $\rho_{pol} \approx -0.45$ a maximum $\tau_{st} = 240ms$ can be reached.

The described possibilities for tailoring the size and repetition rate of sawteeth are very interesting in itself, but also open the possibility to avoid the sawteeth as the main trigger for NTMs at all or destabilise them and get small high frequent sawteeth which are no longer able to trigger NTMs.

2.2. Avoidance of NTMs by sawtooth control The schemes described above for controlling sawteeth have been applied to discharges with significantly higher beam heating power $P_{NBI} = 12.5MW$, reaching high β_N values, with $P_{ECCD} = 1.8MW$, which are vulnerable for NTMs [1]. Discharges with off-axis co-ECCD and on-axis counter-ECCD have been performed in order to fully suppress sawteeth. Both for co- and counter-ECCD sawtooth-free phases are achieved, accompanied by fishbone activity. The fishbone activity can be attributed to an increased fast particle content due to the higher NBI power (fig. 1). The sawtooth behaviour is also modified by the increased NBI heating power and the effects of the ECCD as described above are less pronounced. For the on-axis counter-ECCD case the suppression is not complete and some sawteeth with a very low frequency appear. A magnetic field ramp has been applied to get a resonance of the ECCD at the (1/1) surface. In order to compensate for the Shafranov shift during the field ramp a β-feedback keeps $\beta_N \approx 2.8$ constant. Only in the off-axis co-ECCD case the triggering of an NTM could be avoided for the entire ECCD pulse length of 2 seconds. In the counter-ECCD phase an NTM is triggered by a fishbone during the ECCD pulse. After switching off the co-ECCD immediately an NTM appears triggered by the first sawteeth. In summary, the off-axis co-ECCD scenario seems to be more reliable in suppressing sawteeth as the NTM trigger at high β_N values. At JET similar experiments with ICCD have demonstrated successfully the avoidance of NTMs by sawtooth suppression [5].

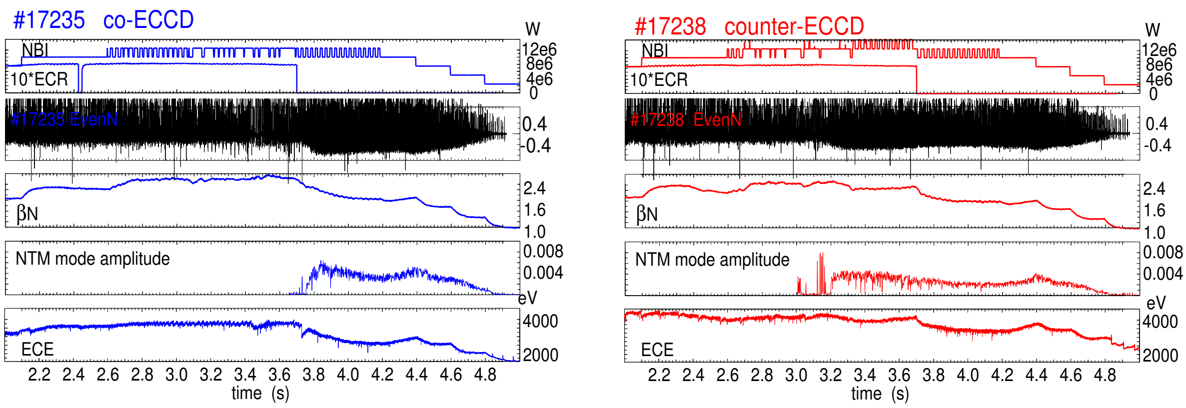

Figure 1: Avoidance of NTM triggering sawteeth for off-axis co-ECCD and on-axis counter-ECCD. During the entire co-ECCD pulse sawtooth could be avoided and no NTM has been triggered. For the the counter-ECCD case an NTM has been triggered during the ECCD pulse by a large fishbone.

3. Stabilisation of NTMs with local co-current drive by ECCD

Not in all cases the excitation of NTMs can be avoided by suppressing its triggering seed-island such as sawteeth. For example, at higher β_N, also fishbones may trigger NTMs. It is therefore highly desirable to develop schemes for stabilising an existing NTM by external means. By replacing the missing equilibrium bootstrap current j_{BS} within the islands O-point, which is the drive for the NTM, by externally driven localised current, it is possible to stabilise both a (3/2)-NTM [6,7], as well as a (2/1)-NTM [8] in ASDEX Upgrade (see fig. 2).

Up to now all NTM stabilisation experiments are done in low triangularity discharges with $I_p = 0.8MA$ and $B_T \approx -2.05$ for the (3/2)-NTM or $-1.85T$ for the (2/1)-NTM and conventional monotonic q-profiles in H-mode. The stabilisation experiment is done, after a short high power phase ($P_{NBI} \approx 15MW$ or $10MW$ for a (2/1) or (3/2)-NTM) to reliably trigger an NTM, during a 3s phase with reduced NBI power. For the (2/1)-NTM this reduction of P_{NBI} is required due to the finite available power in the ECCD. For the (3/2)-NTM the available P_{ECCD} is sufficient to always stabilise the (3/2)-NTM. Due to the hysteresis in β_p of NTMs, they persist with the reduced heating power. The ECCD antennas are used with a toroidal launching angle of -15° for co-ECCD at the corresponding resonant surface with a typical deposition width of $\approx 4-5cm$ (full Gaussian width of j_{ECCD}, see fig. 3). In order to deposit the ECCD at the resonant surface, a magnetic field ramp of $+0.3T$ is included, corresponding to a scan of $\approx 19.8cm$ on the high field side. It typically takes several $100ms$ to stabilise a (3/2) mode during the B_t-ramp. In discharges with a constant optimised magnetic field derived from the B_t-scans the stabilisation typically takes less than $100ms$.

With this scenario the (3/2)-NTM could be stabilised at a maximal $\beta_N \approx 2.6$ with $P_{NBI} = 10MW$. For the (2/1)-NTM a maximal $\beta_N \approx 1.9$ with $P_{NBI} = 6.25$ and $P_{ECCD} = 1.9MW$ could be achieved. The significantly higher required ECCD power for the (2/1)-NTM, together with the lower achievable β_N, can be explained by the reduced ECCD current drive efficiency at lower temperatures T_e and the reduced β_p^{marg} compared to the (3/2)-NTM [9,10].

The (2/1)-NTM is created in non-rotating locked state (grey shaded area in fig. 2). Before the stabilisation the mode must start rotating again or the ECCD power must be deposited in the islands O-point in its locked position. By the reduced NBI power the local β_p is reduced and, since for a saturated NTM $W_{sat} \sim \beta_p$ holds, this reduces the island size and the mode rotates again. This unlocking happens faster in the presence of the ECCD already in this phase. This shows that the possibility to unlock a mode with ECCD, if the alignment is adjusted such, that power is deposited in the O-point of the island.

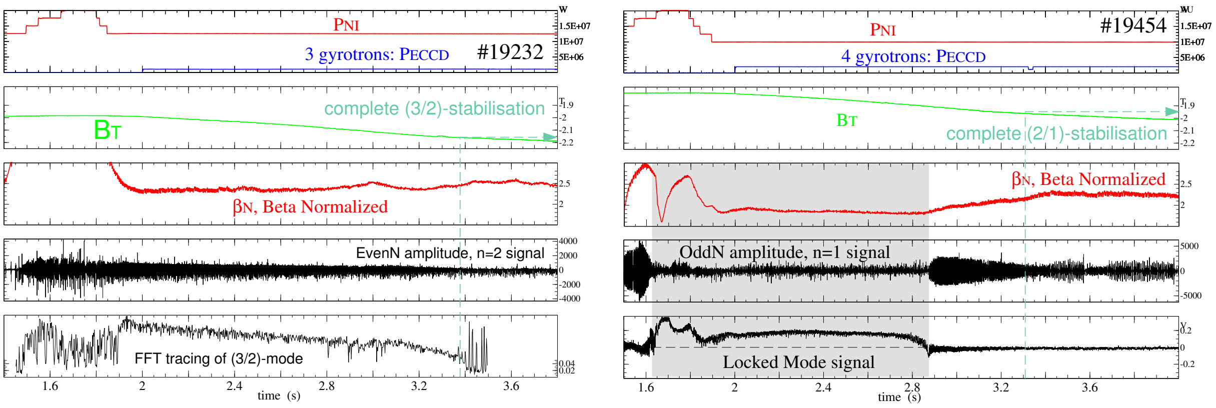

Figure 2: Stabilisation of a (3/2) (left figure) and a (2/1)-NTM (right figure) at high β_N by co-ECCD at the corresponding resonant surface. Note that the (2/1)-NTM is preceeded by a phase (grey shaded) where the mode is locked to the vacuum vessel leeding to a larger loss in confinement.

3.1. Influence of the ECCD deposition width on the stabilisation The experiments described above were done with a deposition width d smaller than the marginal island size W_{marg} ($d < W = W_{marg}$) below which the island decays away independently of β_p. If the island size W is smaller than the ECCD deposition width d while still being larger than the marginal island size W_{marg} ($W < d$ and still $W > W_{marg}$), theory predicts that the required power can be substantially higher. As for ITER W_{marg} might be smaller compared to present experiments, this situation might occur and must be tested by artificially achieving $W < d$. If this is the case, theory predicts that a modulation of the ECCD will be required in order to deposit ECCD power only in the O-point of the island [11].

The suppression efficiency as a function of the ratio between W and a modified deposition width d has been investigated both numerically and experimentally for non-modulated ECCD. Toroidal launching angles of the ECRH antennas between 0° (pure heating) and 25° have been used to vary the amount of the driven current I. For larger angles the current drive efficiency is increasing, whereas the deposition width d is also increasing. ECCD current is driven outside the separatrix of the island for $d > W$. This current is lost for the stabilisation of the mode and only $I \cdot W/d$ contributes. This leads to the definition of the figure of merrit I/d [12].

In the third part of fig. 3 (blue curve) the achievable reduction of the island size due to the ECCD as a function of the toroidal launching angle is shown. The island size reduction is normalised to the island size before applying the ECCD, i.e. $W_{norm} = W_{min}/W_{sat,noECCD}$. The red curve of the third part of fig. 3 shows the calculated driven current normalised to the deposition width, I/d. For small angles $\approx -5°$ a clear maximum in I/d is predicted from these TORBEAM calculations corresponding to the highest current density, although the total driven current increases with angle (see fig. 3). For angles $< -15°$ (broader deposition, reduced I/d) only partial stabilisation is observed. Consistently, angles between $-15°$ and $0°$ (pure heating) show a complete stabilisation ($W_{min}/W_{sat} = 0$), both for 1.0MW and 1.4MW of ECCD power.

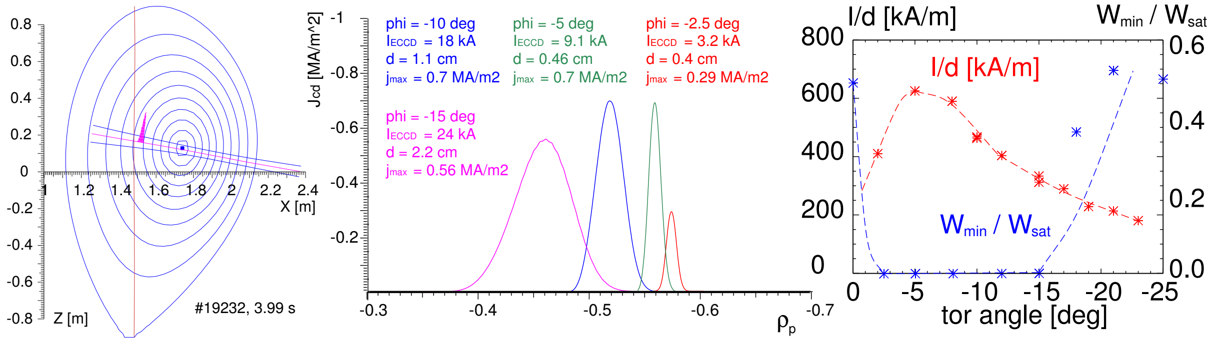

Figure 3: TORBEAM calculations of the localisation, the radial deposition width and the total driven current for different launching angles. The first figure shows the deposition area in a poloidal cross section from ASDEX Upgrade, the second figure the deposition profile for $-15°, -10°, -5°, -2.5°$ toroidal launching angle for constant B_t. The ratio I/d as function of the launching angle (red curve) [12] is shown in the third figure together with the experimentally achieved reduction of the island normalised to the size without co-ECCD (blue curve).

Based on these experiments, the stabilisation scheme has been adopted towards smaller toroidal launching angles with an increased driven current density I/d at the resonant surface. The highest values in achievable β_N and background NBI power shown in fig. 2 were performed with $\approx -5.0°$ launching angle. Again a magnetic field scan has been included to target the resonant surface. For the (3/2)-NTM, $\beta_N = 2.6$ at $P_{NBI} = 12.5MW$ and $P_{ECCD} = 1.0MW$ has been obtained. This increases the achievable ratio between β_N and the P_{ECCD} for the (3/2)-NTM to $\beta_N/P_{ECCD} = 2.6MW^{-1}$. For the (2/1)-NTM stabilisation with increased current density I/d, β_N could be raised from $\beta_N = 1.9$ with $P_{NBI} = 6.25MW$ to $\beta_N = 2.3$ with $P_{NBI} = 10MW$ and a reduction of the required ECCD power from $P_{ECCD} = 1.9MW$ to $P_{ECCD} = 1.4MW$. This results for the (2/1)-NTM in $\beta_N/P_{ECCD} = 1.64MW^{-1}$ compared to originally $\beta_N/P_{ECCD} = 1.0MW^{-1}$

A further increase of the NBI heating power after the removal of the NTM leads to even higher β_N values as long as the ECCD is preventing another excitation. A new NTM gets excited when the ECCD is switched off. Due to the changed Shafranov shift and the resulting misalignment of the ECCD with the resonant surface, a new NTM can get excited at higher β_N.

The presently installed ECRH launchers with a fixed frequency of 140 GHz allow no feedback controlled NTM-stabilisation. An upgrade of the ECRH system with higher power and multifrequency gyrotrons is in progress [11]. Additionally a new set of mirrors is installed with the possibility of a feedback control of the poloidal launching angle during the discharge. With this flexibility, experiments with a feedback for the resonant surface of the NTM are planed in the next year. In preliminary experiments for the feedback control, the radial location of the

NTM as well as the ECCD deposition have been detected simultaneously with ECE measurements [13]. For the localisation of the ECCD the power has been modulated with 90% duty cycle at low frequencies of $f_{ECCD} \approx 40 - 100Hz$. The ECE measurement then also provides the localisation of the deposition.

With this scheme at hand the stabilisation of NTMs in arbitrarily shaped discharges with different q_{95} values is possible and will be addressed in the near future. These technical improvements will also be used for the sawtooth tailoring in the vicinity of the $q = 1$ surface. Especially the ITER hybrid scenario and the improved H-mode are of special interest in this context.

4. Frequently Interrupted Regime NTMs, FIR-NTMs

In the presence of NTMs at high β_N values ($\beta_N > 2.3$) a modified NTM behaviour, the frequently interrupted regime (FIR), has been found and theoretically explained at ASDEX Upgrade and later at JET [14,15]. Due to a non-linear three wave coupling between the (3/2)-NTM, a (1/1) mode and a bursty (4/3) mode the amplitude of the NTM is abruptly reduced [16,17,15]. The amplitude drops only appear, if the three modes are phase locked. This indicates that a three-wave coupling is required for the amplitude drops. For repetition times of these amplitude drops higher than the growth time of the NTM, the average island size never reaches its saturated size W_{sat}. The resulting confinement degradation compared to a saturated NTM is therefore reduced. A significant recovery of the confinement quality H_{98y} for $\beta_N > 2.3$ could be established at ASDEX Upgrade and JET (see fig. 4).

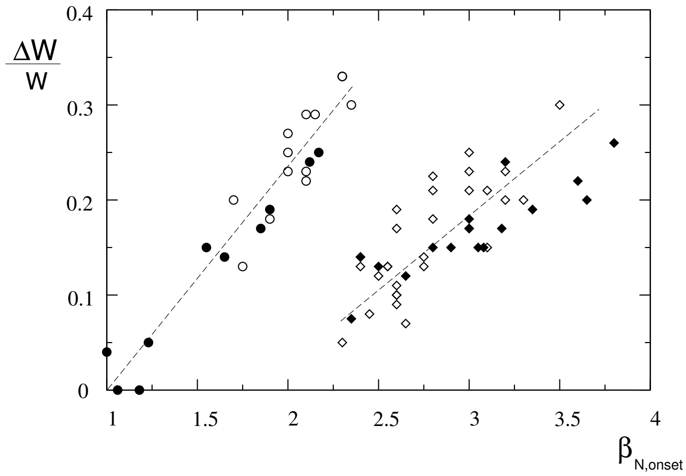

Figure 4: Confinement degradation (loss in plasma energy ΔW normalised to plasma energy at the onset W) of saturated NTMs (circles) and FIR-NTMs (diamonds) for ASDEX Upgrade (open symbols) and JET (full symbols) [15] as function of $\beta_{N,onset}$. Good agreement for the FIR-NTM regime for $\beta_N > 2.3$ is seen. For JET the effect of ELMs is ignored.

For JET already a reduction in the confinement loss due to the NTM at $\beta_N = 1.9$ can be observed (fig. 2 and 3 in [15]). The range of $1.9 < \beta_N < 2.5$ is characterised by small toroidal fields and small q_{95} ($B_t < 1.2T$ and $q_{95} \simeq 2.5$). High β_N values could be achieved with small NBI heating powers. In this case the heating power could just trigger the transition form type III to type I ELMs. Large infrequent type I ELMs are responsible for the amplitude drops in the NTM leading to a reduction of the confinement loss with an entirely different mechanism (fig. 2 in [15]).

4.1. The physics and triggering of FIR-NTMs

The short growth time of the (4/3) mode, typically less than $200\mu s$, its duration of $1ms$ and the required high pressure suggests this mode to be an ideal mode close to its marginal limit. Detailed stability calculations for this type of ideal (4/3) mode show a clear destabilisation with increasing pressure gradient dp/dr and with decreasing local shear $dq/dr \cdot r/q$ at the (4/3) surface [15]. Such a behaviour is described for the so-called infernal mode [18], and appears normally in internal transport barriers, where it is driven by the large pressure gradient at the location of the barrier.

Local current drive close to the (4/3) surface reduces the local shear and should therefore destabilise this type of mode. In discharges with $\beta_N \approx 2.4$ without an NTM it has been shown that ideal (4/3) modes with co-ECCD just outside the (4/3) surface can be triggered. A resulting reduction of the local shear by the co-ECCD is thought to be responsible for triggering this mode. Combined TORBEAM and ASTRA calculation give a reduction in the local shear within the ECCD deposition of 0.15-0.3. The fast growth and decay time of this mode is consistent with its ideal character. In addition, for a constant monotonic current profile and hence a constant shear, the required high pressure for achieving a FIR-NTM, reflected by the requirement $\beta_N >$ 2.3, can be explained by these requirements for the existence of the (4/3) mode.

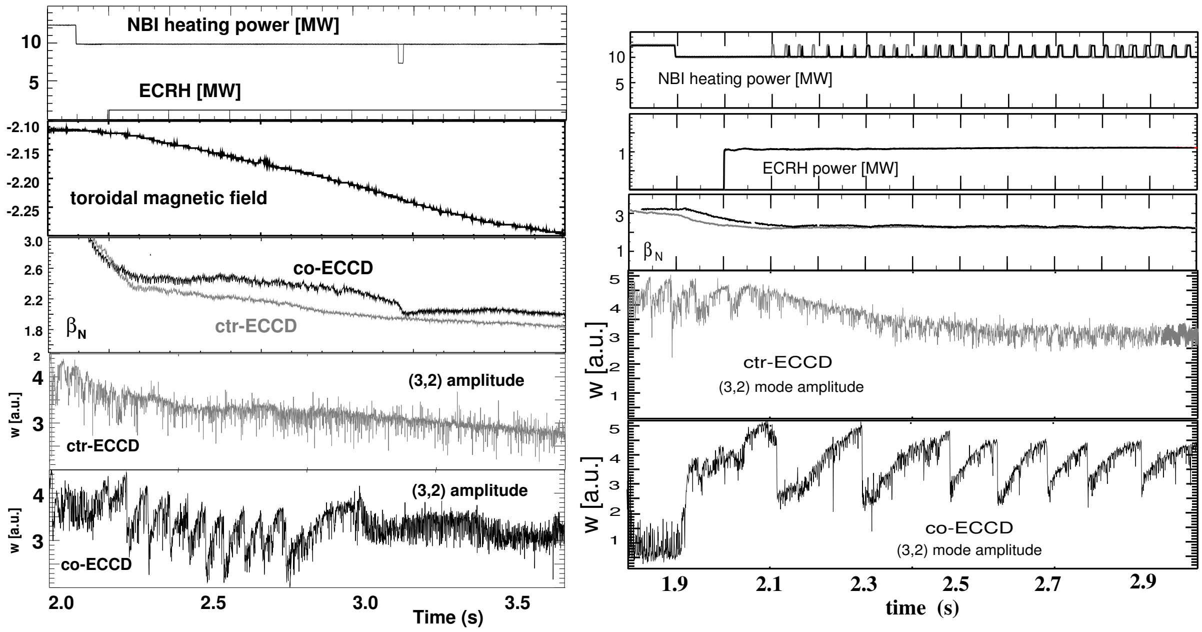

Figure 5: Left figure: Time traces of P_{NBI}, P_{ECCD}, B_t, β_N and the (3/2) amplitude from magnetics with co- and counter-ECCD (#17950, black and #17949, grey). The toroidal field scan give the optimal magnetic field B_t for triggering a FIR-NTM in the co-ECCD case. For counter-ECCD no FIR behaviour could be observed. Right figure: With the optimal field of $B_t = -2.19$ T only in the co-ECCD case (#17955, black) a FIR-NTM could be triggered. In the counter-ECCD case (#17956, grey) the FIR-behaviour disappears with the application of the ECCD. The FIR-behaviour is more pronounced with co-ECCD at constant magnetic field.

Applying co or counter-ECCD in the vicinity of or just outside the (4/3) surface, a triggering or suppression of a FIR-NTM is possible destabilising or stabilising the (4/3) mode. With a decrease / increase of the shear just outside the resonant surface by co / counter-ECCD the (4/3) mode can be triggered or suppressed and the FIR-NTM can be artificially induced or suppressed (see fig. 5). For a reliable modification of the shear in one discharge again a toroidal field ramp towards higher fields has been used. For this experiment the starting field is slightly increased in order to start depositing inside the (3/2) surface on the high field side and hit the (4/3) surface during the scan. As expected for co-ECCD the FIR-NTM can be triggered and the for counter-ECCD no FIR-behaviour is observed. Using a constant optimal field of $B_T = -2.19T$ taken from these discharges (see the left part of fig. 5) the effect is even more pronounced. The amplitude drops of the (3/2)-NTM are much stronger for a decrease of the shear. The FIR-behaviour is suppressed for an increase of the shear for similar β_N-values.

4.2. FIR-NTMs in ITER relevant scenarios The consideration of the local shear in the previous section can be extended to a more global consideration of the global shear in the plasma centre. The so-called improved H-mode at ASDEX Upgrade as well as the ITER hybrid scenario has a flat central shear with $q \approx 1$ in the plasma centre. At ASDEX Upgrade the flat shear is achieved by early preheating with the NBI during the current rise phase. At JET the hybrid scenario is achieved by applying lower hybrid current drive during this phase. The flat shear region makes it easier to trigger in both scenarios the required (4/3) mode for the transition of an NTM to a FIR-NTM. At JET for low $q_{95} \approx 3.5$ ($I_p = 1.0MA, B_t = 1.2T$) a clear FIR-NTM can be observed together with high $\beta_N = 3.3$ and good confinement ($H_{98y} = 1.4$). By avoiding a $q = 1$ surface (higher B_t and q_{95}) a modification with a continuous (4/3) mode can be achieved. Both the (3/2)-NTM and the (4/3) mode have small amplitudes in this scenario and one can reach good confinement ($H_{98y} = 1.5$) and high pressure ($\beta_N = 2.9$).

The natural low global shear or artifically ECCD triggered low local shear show a route how to optimise scenarios to reach high β_N values in the presence of NTMs, if they can not be avoided or suppressed by external means. The local ECCD plays a central role in this context.

5. Summary and conclusions

In ASDEX Upgrade the repetition rate and size of sawteeth has been modified by local co and counter-ECCD. Full suppression of sawteeth has been proven for the maximum ECCD duration of 2 seconds for on-axis counter ECCD and off-axis co-ECCD. The sawteeth behaviour can be explained with the variation of the $q\prime$ at the $q = 1$ surface. At higher β_N the excitation of NTMs could be avoided with this sawteeth suppression scheme.

The stabilisation of NTMs by local current drive at the resonant surface with ECCD has been extended at ASDEX Upgrade for (2/1)-NTMs. The achievable β_N for both types of NTMs has been increased by optimising the deposition width and driven current. For the (3/2)-NTM the achievable $\beta_N = 2.6$ at the stabilisation could be achieved with $\beta_N/P_{ECCD} = 2.6MW^{-1}$. The (2/1)-NTM could be stabilised at $\beta_N = 2.3$ with $\beta_N/P_{ECCD} = 1.64MW^{-1}$.

With local co and counter current drive at the (4/3) surface the triggering of an ideal (4/3) mode opens the possibility to trigger artificially at lower β_N or suppress at high β_N the so-called FIR-NTM regime with a reduced confinement degradation. The analysis of these artificially triggered FIR-NTMs provided the key understanding for this scenario.

For all three approaches (NTM avoidance by seed-island suppression, active NTM stabilisation, triggering of FIR-NTMs) the enhancements at ASDEX Upgrade and the ECRH system provide central tools. The use of a feedback control system for the deposition of the ECCD by steerable mirrors, combined with step tunable gyrotrons, will give much more flexibility.

References

[1] MÜCK, A. et al., in *30th EPS Conf., St. Petersburg*, volume 27A, page P1.131, 2003.
[2] MÜCK, A. et al., to be subm. to Plasma Phys. Controlled Fusion (2004).
[3] POLI, E. et al., Comput. Phys. Commun. **136** (2001) 90.
[4] ANGIONI, C. et al., Nucl. Fusion **43** (2003) 455.
[5] SAUTER, O. et al., Phys. Rev. Lett. **88** (2002) 105001.
[6] GANTENBEIN, G. et al., Phys. Rev. Lett. **85** (2000) 1242.
[7] GANTENBEIN, G. et al., in *29th EPS Conf., Montreux*, volume 26B, page P1.036, 2002.
[8] GANTENBEIN, G. et al., in *30th EPS Conf., St. Petersburg*, volume 27A, page P1.187, 2003.
[9] MARASCHEK, M. et al., Plasma Phys. Controlled Fusion **45** (2003) 1369.
[10] MARASCHEK, M. et al., in *30th EPS Conf., St. Petersburg*, volume 27A, page P1.120, 2003.
[11] LEUTERER, F. et al., Fusion Eng. Design **66–68** (2003) 537.
[12] ZOHM, H. et al., to be subm. to Phys. of Plasmas (2004).
[13] KELLER, A. et al., in *30th EPS Conf., St. Petersburg*, volume 27A, page P1.130, 2003.
[14] GÜNTER, S. et al., Nucl. Fusion **43** (2003) 161.
[15] GÜNTER, S. et al., Nucl. Fusion **44** (2004) 524.
[16] GUDE, A. et al., Nucl. Fusion **42** (2002) 833.
[17] GÜNTER, S. et al., Phys. Rev. Lett. **87** (2001) 275001.
[18] MANICKAM, J. et al., Nucl. Fusion **27** (1987) 1461.